

# Accurate description of bulk and interfacial properties in colloid-polymer mixtures

R. L. C. Vink,<sup>1</sup> A. Jusu,<sup>2</sup> J. D. Zubiella,<sup>3</sup> and C. N. Likos<sup>4</sup>

<sup>1</sup>Institut für Physik, Johannes-Gutenberg-Universität, Staudinger Weg 7, D-55099 Mainz, Germany

<sup>2</sup>Lehrstuhl für Physikalische Chemie I, Universität Bayreuth, D-95440 Bayreuth, Germany

<sup>3</sup>NSF Center for Theoretical Biological Physics (CTBP), Department of Chemistry and Biochemistry, University of California, San Diego, La Jolla, California 92093-0365

<sup>4</sup>Institut für Theoretische Physik II, Heinrich-Heine-Universität Düsseldorf, D-40225 Düsseldorf, Germany  
(Dated: March 23, 2024)

Large-scale Monte Carlo simulations of a phase-separating colloid-polymer mixture are performed and compared to recent experiments. The approach is based on effective interaction potentials in which the central monomers of self-avoiding polymer chains are used as effective coordinates. By incorporating polymer nonideality together with soft colloid-polymer repulsion, the predicted binodal is in excellent agreement with recent experiments. In addition, the interfacial tension as well as the capillary length are in quantitative agreement with experimental results obtained at a number of points in the phase-coexistence region, without the use of any fit parameters.

PACS numbers: 82.70.Dd, 61.20.Ja, 82.70.-y

In addition to commercial applications, mixtures of colloids and nonadsorbing polymer are interesting because of their analogy to atomic systems [1]. Much effort has been devoted to understand the phase behavior of such mixtures. Of particular interest is phase separation, which occurs when the polymer density and diameter of gyration are sufficiently large, leading to the formation of two coexisting phases: one phase lean in colloids and dense in polymers (the colloidal vapor) and one phase dense in colloids and lean in polymers (the colloidal liquid). As was shown by Asakura and Osawa (AO), phase separation in colloid-polymer mixtures (CPM) is driven by entropy [2]. In the AO description, colloids and polymers are treated as effective spheres, assuming hard-sphere interactions between colloid-colloid and colloid-polymer pairs, while the polymers can interpenetrate freely. A major advance has been the development of a geometry-based density functional for the AO model [3], which has led to a host of novel and intriguing predictions regarding interfacial phenomena within this model [4]. However, when comparing to actual experiments, quantitative discrepancies arise. An important deviation of the AO model is that it underestimates the polymer concentration in the colloidal liquid [5, 6]. This effect is more pronounced within the free-volume approximation [7], which is also the bulk limit of the density functional of Ref. [3], and it persists when the AO binodals are obtained by means of computer simulations [5, 8].

While the colloid-colloid interaction in realistic systems is indeed well described by the hard sphere potential [9], the colloid-polymer and polymer-polymer interactions are more complex. To circumvent the shortcomings of the AO model, numerous different approaches have been employed, both at the effective [10, 11, 12, 13] and at the monomer-resolved [14, 15] levels. As a general trend, inclusion of polymer nonideality does improve on the major drawback of the AO model, i.e., it yields higher polymer concentrations in the colloidal liquid [11, 13]. A remarkably accurate method to capture polymer nonide-

ality is the "polymer as soft colloid" approach [16]. Here, the polymers' centers of mass are chosen as effective coordinates while all fluctuating monomers are canonically integrated out. The sought-for effective potentials are obtained by inverting the correlation functions obtained in Monte Carlo (MC) simulations of self-avoiding random walks (SAW) on a lattice [16, 17, 18]. The pioneering work of Bolhuis et al. [18] has led to the most accurate determination of the phase behavior of CPM to date, demonstrated by direct comparison to experiments [5].

Despite the progress in calculating bulk phase diagrams, accurate predictions of the interfacial tension between coexisting phases, a quantity that plays a key role in wetting and interfacial phenomena, remain elusive. Theoretical approaches include the square-gradient approximation [6, 19, 20], density-functional theory [15, 21, 22] and simulations [8, 12, 23]. Experimental data on  $\gamma$  are hard to obtain, mainly due to the very small value of this quantity ( $\sim 1$  N/m). In several cases [6, 19, 21], theoretical predictions have been compared to the experimental results of Refs. [24] and [25]. These comparisons are carried out by plotting the theoretical interfacial tension as a function of the colloid density gap across the binodal, a procedure that tends to obscure the fact that the theoretical and experimental binodals can be in considerable disagreement [6]. Recently, Moncho-Jorda et al. [22] employed density-functional theory to calculate the interfacial tension employing the interactions of Ref. [5]. However, they adopted a depletion picture, losing thereby the effect of polymer-induced many-body interactions between the colloids. Thus, a full two-component treatment of interacting CPM is necessary in order to capture bulk and interfacial behavior quantitatively [22].

In this Letter, we demonstrate that simulations of CPM using accurate effective interactions predict bulk and interfacial properties correctly. We consider the so-called "colloid limit", where the polymer diameter of gyration  $\sigma_g$  is smaller than the colloid diameter  $\sigma_c$ . Re-

cently, experimental measurements of the interfacial tension and capillary length in the colloid limit became available, to which we can compare [26]. At the same time, accurate effective interactions for the colloid limit exist, obtained in off-lattice molecular dynamics (MD) simulations of self-avoiding polymer chains [27]. We choose here the central monomer to represent the chain, canonically tracing out the remaining, fluctuating monomers. If the coarse-graining procedure is carried out accurately, the bulk thermodynamics of the mixture should be strictly independent of the choice of the effective coordinates [28]. Moreover, for athermal solvents and in the limit of long chains, details of the microscopic monomer-monomer in-

teractions become irrelevant [29]. Thus, the phase behavior should be independent of whether one adopts for the polymers a lattice, SAW model as done in Ref. [5], or the approach at hand. We will explicitly check whether this requirement is fulfilled in what follows.

The colloids are represented by their centers and  $r$  denotes the distance between any effective coordinates in the corresponding effective interactions  $V_{ij}(r)$ , with  $i, j = c, p$ . The colloid-colloid interaction  $V_{cc}(r)$  is given by a hard-sphere potential of diameter  $\sigma_c$ . The colloid-polymer interaction,  $V_{cp}(r)$  diverges for  $r < \sigma_c/2$  and for larger separations it reads as [27]:

$$V_{cp}(r) = \begin{cases} \frac{\sigma_c^2}{2r} & \text{if } r < \frac{\sigma_c}{2} \\ \frac{1}{2} \ln \frac{2r - \sigma_c}{\sigma_p} & \text{if } \frac{\sigma_c}{2} < r < \frac{\sigma_c + \sigma_p}{2} \\ \frac{1}{2} \frac{\text{erf}(\frac{2r - \sigma_c}{\sigma_p})}{1 - \text{erf}(\frac{\sigma_p}{\sigma_p})} & \text{if } r > \frac{\sigma_c + \sigma_p}{2} \end{cases}$$

where  $\sigma_p$  a typical length scale given by  $\sigma_p = 0.66 \sigma_c$ ,  $\sigma_c = (k_B T)^{-1}$ ,  $T$  the temperature,  $k_B$  the Boltzmann constant,  $\sigma_p = \sigma_c (1 + \frac{1}{2} \frac{\sigma_c^2}{\sigma_p^2})$ ,  $\sigma_p = \sigma_c (1 - \frac{1}{2} \frac{\sigma_c^2}{\sigma_p^2})$   $\exp(\frac{1}{2} \frac{\sigma_c^2}{\sigma_p^2})$ , and parameters  $\sigma_c$  and  $\sigma_p$ , determined in Ref. [27] by fitting to simulation results. The corresponding polymer-polymer interaction is given by:

$$V_{pp}(r) = 0.786 \begin{cases} \ln \frac{r}{\sigma_p} + \frac{1}{2} \frac{\sigma_c^2}{\sigma_p^2} & \text{if } r < \sigma_p \\ \frac{1}{2} \frac{\sigma_c^2}{\sigma_p^2} \exp(-\frac{1}{2} \frac{\sigma_c^2}{\sigma_p^2} (r^2 - \sigma_p^2)) & \text{if } r > \sigma_p \end{cases}$$

with  $\sigma_p$  obtained by requiring that the effective interaction correctly reproduces the second virial coefficient of dilute polymer solutions and resulting in the value  $\sigma_p = 1.03$  [27]. To match the experiment of Ref. [26], we consider a mixture of colloids and polymers with size ratio  $q = \sigma_c = 0.56$ . The parameters are  $\sigma_c = 0.46$ , and  $\sigma_p = 0.52715$  [30].

The binodal and the interfacial tension are obtained in the grand canonical ensemble, by MC simulation of a mixture of  $N_c$  colloids and  $N_p$  polymers, interacting via the above pair potentials. In this ensemble, the temperature, the volume  $V$ , and the respective fugacities,  $z_c$  and  $z_p$ , of colloids and polymers, are fixed, while the number of particles in the system fluctuates. We also introduce the colloid and polymer packing fractions  $\phi_{c,p} = (\frac{4}{3} \pi \sigma_{c,p}^3 / 6) N_{c,p} / V$ . Since the interactions are athermal, the temperature plays no role and the phase behavior is set by  $q$  and the fugacities. The polymer fugacity is used as control parameter, analogous to inverse temperature in fluid-vapor transitions in atomic systems. For a given  $z_p$ , we measure the distribution  $P(\phi_c)$ , defined as the probability of observing a system with colloid packing fraction  $\phi_c$ . For  $z_p$  sufficiently far away from the critical point, phase coexistence is obtained by tuning  $z_c$  so that  $P(\phi_c)$  becomes bimodal, with two peaks of equal

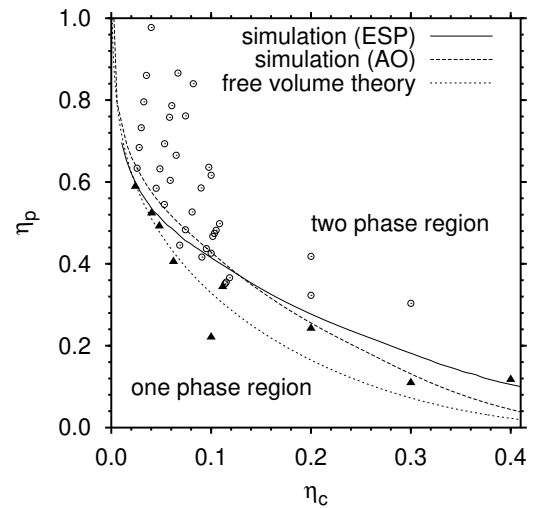


FIG. 1: Colloid-polymer binodals for  $q = 0.56$  obtained in simulations using two different models (ESP and AO). Open circles are experimental state-points at which phase separation was observed; black triangles are experimental state-points at which only one phase was observed. The experimental data were taken from Refs. [26] and [33]. The free-volume AO-binodal is also shown.

area. The peak at low  $\phi_c$  corresponds to the colloidal vapor phase, the peak at high  $\phi_c$  to the colloidal liquid, and the region in between to phase-separated states [8]. The average peak locations yield the colloid packing fractions in the two phases. The interfacial tension is obtained from the average height of the peaks [8, 31]. In order to simulate efficiently, a grand canonical cluster move is used [8], in combination with a reweighting scheme [32].

To obtain the binodal, we vary  $z_p$  and record the cor-

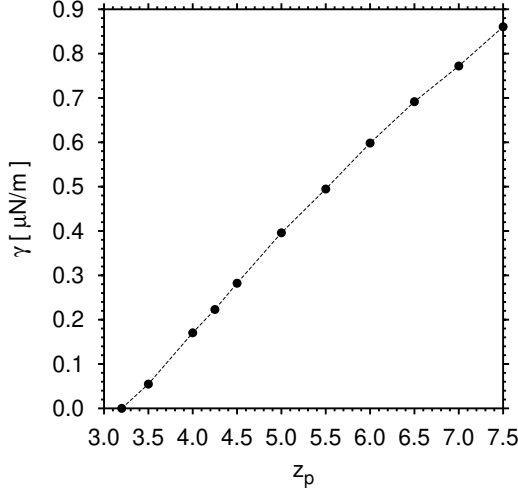


FIG. 2: Interfacial tension against the polymer fugacity from our ESP-simulations. The line is a guide to the eye.

responding densities of colloids and polymers in the two coexisting phases. This yields the phase diagram in system representation, which may directly be compared to experiments, see Fig. 1. The solid curve is the binodal of the present work incorporating the effective soft potentials (ESP)  $V_{cp}(r)$  and  $V_{pp}(r)$  above. For comparison, the dashed line shows the binodal of the AO model with  $q = 0.56$ , obtained following the same grand canonical simulation procedure. The free volume result is also shown. As seen in Fig. 1, ESP interactions give an accurate description of the experimental binodal. Note in particular the significant increase in the polymer density at high colloid density in comparison to the AO-result.

Next, we consider the interfacial tension, and compare to the recent experiment of Ref. [26]. The colloids are PMMA spheres ( $\sigma_c = 50$  nm), mixed with polymer with diameter of gyration  $\sigma_g = 28$  nm, and dissolved in decalin at  $T = 298$  K. In Fig. 2, we show simulation results of the interfacial tension as function of  $z_p$ . As expected, the tension decreases markedly upon lowering  $z_p$ , vanishing at the critical point (the critical polymer fugacity is approximately  $z_{p,cr} = 3.2$ ). To enable the comparison to experiment, we show in Fig. 3 several binodal tielines obtained in the simulation. At point X, which is close to the tieline corresponding to  $z_p = 4.25$ , the experimental interfacial tension equals  $\gamma = 0.16 \pm 0.2$  N/m [26]. The corresponding interfacial tension in the simulation reads  $\gamma = 0.22$  N/m, which exceeds the experiment by only 10%. In contrast, the interfacial tension obtained at the same state-point in a simulation of the AO model is  $\gamma = 0.07$  N/m, which underestimates the experiment by over 50%. This is due to subtle differences in the location and range of the critical regions of the two models. More precisely, dening the distance from the critical point as  $z_p = z_{p,cr} + 1$ , we obtain for point X using ESP interactions  $t = 0.33$ , but only  $t = 0.05$  using the

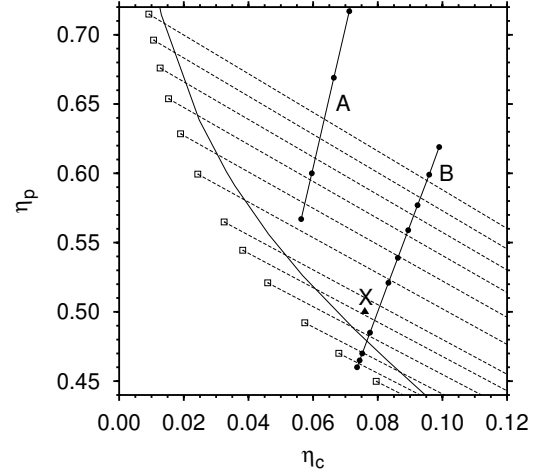


FIG. 3: Close-up of the vapor branch of the binodal. Open squares with tielines (dashed) are binodal points obtained using ESP interactions. The polymer fugacity corresponding to the tielines reads  $z_p = 7.5 : 7 : 6.5 : 6 : 5.5 : 5 : 4.5 : 4.25 : 4 : 3.75 : 3.5 : 3.45$  (from top to bottom). The solid curve is the binodal of the AO model. The X-symbol ( $\eta_c = 0.076$ ,  $\eta_p = 0.50$ ) marks a state-point at which the interfacial tension was measured experimentally. The closed circles on the dilution lines A and B are experimental state-points at which the capillary length was measured.

AO model. For the AO model, point X is thus much closer to criticality and hence the interfacial tension is lower. At the same time, if one calculates the interfacial tension for the AO model using the free volume tieline with the same colloid density gap as in the experiment, the value  $\gamma = 0.5$  N/m is obtained [26]. These discrepancies within the AO model demonstrate the large effect that inaccuracies in the binodals have on  $\gamma$ , as well as ambiguities that arise by comparing interfacial tensions at "rescaled" state-points. In our approach, on the contrary, we provide a comparison to the experimentally measured interfacial tension in absolute terms, i.e., at the same state-point ( $\eta_c; \eta_p$ ).

Finally, we compare to experimental measurements of the capillary length  $l_c = \sqrt{\gamma / (\rho_l - \rho_v)g}$ , with  $g = 9.81$  m/s<sup>2</sup> the gravitational acceleration, interfacial tension  $\gamma$ , and  $\rho$  the mass density difference between the colloidal liquid and vapor phase. For two coexisting phases with colloid- and polymer-packing fraction gaps  $\phi_c$  and  $\phi_p$  respectively, it holds  $\rho = \phi_c(\rho_c - \rho_d) + \phi_p \rho_p = \rho_p$ , with the mass densities  $\rho_c = 1170$  kg/m<sup>3</sup> for PMMA and  $\rho_d = 890$  kg/m<sup>3</sup> for decalin,  $\rho_p = 3.87 \cdot 10^{22}$  kg the single polymer mass, and  $\phi_p = \frac{3}{6} = 0.5$  the effective single polymer volume [26]. In Fig. 4, we plot the capillary length as obtained in the simulation as function of  $z_p$ . The experimental data are also shown, where the conversion to  $z_p$  was performed with the aid of Fig. 3 (experimental measurements at  $z_p > 7.5$  were converted using linear extrapolation). As  $\rho = \rho_l - \rho_v$  and since

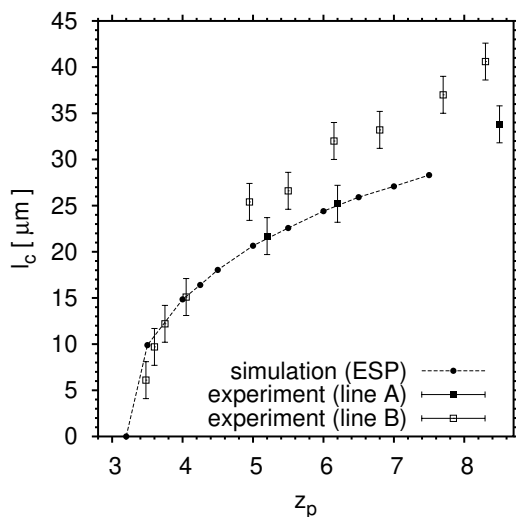


FIG. 4: Capillary length as function of the polymer fugacity obtained in simulations (ESP), as well as in experiments along dilution lines A and B of Fig. 3. The line connecting the simulation data serves as a guide to the eye.

% is given accurately by our approach (as shown by the good agreement with the experimental binodal), the agreement with experiment regarding  $l_c$  directly implies agreement with the interfacial tension at all considered state-points. Another striking feature of Fig. 4 is the remarkably good agreement between simulation and ex-

periment close to the critical point. For 3D Ising systems, the capillary length is expected to vanish at criticality as  $l_c \propto t$  with the critical exponent  $\nu = 2/3$ . While the present simulation and experimental data are not accurate enough to extract the exponent, the curvature of the data is certainly compatible with the anticipated exponent. In particular, the data seem to approach the  $z_p$  axis with perpendicular slope.

In summary, we have demonstrated that the "polymer as soft colloid" approach [16], using accurate effective colloid-polymer and polymer-polymer interactions, not only reproduces the experimental binodal, but also the interfacial tension and the capillary length. Note that excellent agreement with the experimental binodal was also obtained in Ref. [5], in which the polymer centers-of-mass were employed as effective coordinates. Both the effective description of Ref. [5], and the one adopted here, thus reproduce the correct thermodynamics, providing a strong confirmation of the power and self-consistency of coarse-graining techniques. We anticipate that a full, two-component calculation of the interfacial tension using the effective interactions of Ref. [5] will also capture the interfacial properties correctly; the latter should be the subject of further investigations. Additional experimental work in measuring interfacial tensions in colloid-polymer mixtures is also highly desirable.

We thank Dirk Aarts for helpful discussions. This work was supported by the DFG through the SFB-TR 6. Allocation of computer time on the JUMP at the Forschungszentrum Jülich is gratefully acknowledged.

- 
- [1] W. Poon, *Science* 304, 830 (2004).
  - [2] S. Asakura and F. Oosawa, *J. Chem. Phys.* 22, 1255 (1954).
  - [3] M. Schmidt et al., *Phys. Rev. Lett.* 85, 1934 (2000).
  - [4] J. M. Brader et al., *Mol. Phys.* 101, 3349 (2003).
  - [5] P. G. Bolhuis et al., *Phys. Rev. Lett.* 89, 128302 (2002).
  - [6] D. G. A. L. Aarts et al., *J. Chem. Phys.* 120, 1973 (2004).
  - [7] H. N. W. Lekkerkerker et al., *Europhys. Lett.* 20, 559 (1992).
  - [8] R. L. C. Vink and J. Horbach, *J. Chem. Phys.* 121, 3253 (2004).
  - [9] A. Imhof and J. K. G. Dhont, *Phys. Rev. Lett.* 75, 1662 (1995).
  - [10] P. B. Warren et al., *Phys. Rev. E* 52, 5205 (1995).
  - [11] M. Schmidt et al., *J. Chem. Phys.* 118, 1541 (2003).
  - [12] R. L. C. Vink and M. Schmidt, *cond-mat/0501037*.
  - [13] M. Schmidt and M. Fuchs, *J. Chem. Phys.* 117, 6308 (2002).
  - [14] M. Fuchs and K. S. Schweizer, *Phys. Rev. E* 64, 021514 (2001); *J. Phys.: Condens. Matter* 14, R239 (2002).
  - [15] P. Bryk, *J. Chem. Phys.* 122, 064902 (2005).
  - [16] A. A. Louis et al., *Phys. Rev. Lett.* 85, 2522 (2000).
  - [17] P. G. Bolhuis et al., *J. Chem. Phys.* 114, 4296 (2001).
  - [18] P. G. Bolhuis and A. A. Louis, *Macromolecules* 35, 1860 (2002).
  - [19] J. M. Brader and R. Evans, *Europhys. Lett.* 49, 678 (2000).
  - [20] A. Moncho-Jorda et al., *J. Chem. Phys.* 119, 12667 (2003).
  - [21] J. M. Brader et al., *J. Phys.: Condens. Matter* 14, L1 (2002).
  - [22] A. Moncho-Jorda et al., *J. Phys. Chem. B* 109, 6640 (2005).
  - [23] A. Fortini et al., *cond-mat/0501134*.
  - [24] E. H. A. de Hoog and H. N. W. Lekkerkerker, *J. Phys. Chem. B* 103, 5274 (1999).
  - [25] D. G. A. L. Aarts et al., *J. Phys.: Condens. Matter* 15, S245 (2003).
  - [26] D. G. A. L. Aarts, *J. Phys. Chem. B* 109, 7407 (2005).
  - [27] A. Jusuf et al., *J. Phys.: Condens. Matter* 13, 6177 (2001).
  - [28] C. N. Likos, *Phys. Rep.* 348, 267 (2001).
  - [29] P. G. de Gennes, *Scaling Concepts in Polymer Physics*, Cornell University Press (Ithaca, NY, 1979).
  - [30] The value of  $\rho_p$  quoted in Ref. [27] is slightly higher. Extensive additional MD simulations revealed that a lower value of  $\rho_p$  yields a better fit to MD data.
  - [31] K. Binder, *Phys. Rev. A* 25, 1699 (1982).
  - [32] P. Vimala and M. Müller, *J. Chem. Phys.* 120, 10925 (2004).
  - [33] S. M. Jett et al., *Phys. Rev. E* 51, 1344 (1995).